sustainability

MDPI

Article

Coordinated Optimal Operation Method of the Regional Energy Internet

Rishang Long [1,*], Jian Liu [2], Chunliang Lu [3], Jiaqi Shi [1] and Jianhua Zhang [1]

[1] State Key Laboratory of New Energy Power System, North China Electric Power University, Beijing 102206, China; 1142101016@ncepu.edu.cn (J.S.); jhzhang001@ncepu.edu.cn (J.Z.)
[2] School of Electrical and Electronic Engineering, North China Electric Power University, Baoding 071000, Hebei, China; HDLDH@ncepu.edu.cn
[3] State Grid Zhejiang Electric Power Company, Hangzhou 310007, Zhejiang, China; lu_chunliang@zj.sgcc.com.cn
* Correspondence: 1152201118@ncepu.edu.cn

Academic Editors: Shuhui Li and Marc A. Rosen
Received: 22 March 2017; Accepted: 15 May 2017; Published: 19 May 2017

Abstract: The development of the energy internet has become one of the key ways to solve the energy crisis. This paper studies the system architecture, energy flow characteristics and coordinated optimization method of the regional energy internet. Considering the heat-to-electric ratio of a combined cooling, heating and power unit, energy storage life and real-time electricity price, a double-layer optimal scheduling model is proposed, which includes economic and environmental benefit in the upper layer and energy efficiency in the lower layer. A particle swarm optimizer–individual variation ant colony optimization algorithm is used to solve the computational efficiency and accuracy. Through the calculation and simulation of the simulated system, the energy savings, level of environmental protection and economic optimal dispatching scheme are realized.

Keywords: energy internet; coordinated optimal operation; heat-to-electric ratio; energy storage

1. Introduction

Energy shortages, environmental pollution and climate change are important factors restricting the sustainable development of the world, and the corresponding energy and environmental problems have become a major strategic issue of great concern at home and abroad. The development of the energy internet (EI) has become one of the key ways to solve these problems [1–4]. Since Jeremy Rifkin put forward the concept, the EI has been widely discussed around the world. The concept highlights that future energy consumption should take full account of electricity, heat, gas and other forms of energy coupling [5]. In addition to the coordination and intensive use of multiple types of energy through the information system, another important feature of the EI is that the process of energy production, flow, and consumption becomes considerable and controllable [6,7].

At present, there are some preliminary studies in the field of EI, including the research framework [8], the key technology [9], the planning and operation [10–12], prognostic [13–15], and network security [16]. References 8 and 9 summarize the technical structure and the key technology of the EI, which provides some considerations for related field research; prognostic areas include power prediction, predictive diagnosis, and predictive control. In [13], predictive control is applied to the optimized control of the microgrid to achieve the optimal online scheduling. In [14,15], predictive diagnosis is modeled in uninterruptible power supplies and a transformer fault. However, there is no relevant research on the EI, which is perhaps a hot topic for further research. The network structure of the EI is very complex, and network security is another important research direction. Reference [16] has studied the network architecture, security issues, and hardware implementation of a smart grid, dealing with its security aspects and showing solutions for the realization of a wireless network.

The optimal operation strategy is the key factor to achieve the benefits of the EI. However, there is a big difference between EI scheduling and traditional power system scheduling. First of all, there are strong random factors in the power side of renewable energy output and the user side of the load demand, which increase the uncertainties of the scheduling process. Secondly, the system can provide electricity and heat for the users simultaneously, and there is a coupling relationship between the electricity and heat—how to combine the demand of heat and electric load, and the operation constraint of the energy storage (ES) will be a complex decision problem. Finally, there exists a two-way interaction between the regional EI and the external power system. Under the electricity market environment, the EI decision makers need to adjust the power generation plan according to the incentive of different electric power markets to ensure the maximum operation efficiency of the system.

To date, some scholars have carried out relevant research. In [10], the energy flow and information flow characteristics of the EI are analyzed, and the operation mechanism of a dynamic multi-agent system is established with the aim of minimizing the cost of energy supply. However, there is a lack of discussion on the combined cooling, heating and power (CCHP) unit in the model. In [17], the regional integrated energy system optimization scheduling method is established with the aim of economic and environmental protection, and the load-scene classification is optimized, but the function of the ES is not taken into account. In [18], a three-level cooperative global optimization method is proposed, but it is difficult to ensure energy efficiency and the complete decoupling of heat/electricity by using a CCHP unit with a constant heat-to-electric ratio (HTER). In [19,20], energy efficiency is used as a goal to establish an optimization model. In [19], a demand response (DR) program is considered as one of the most cost-effective energy alternatives, and in [20] the development of a CCHP strategy is established to achieve energy efficiency.

The current research is more one-sided, which is mainly reflected in the following ways: (1) The existing analog system is incomplete; a complete regional EI should include multiple types of load (especially heat and cold loads), multi-power (wind turbine (WT), photovoltaic (PV), CCHP, etc.) and ES; (2) CCHP units use a constant HTER strategy, leading to the power and the load not matching, and affecting the system's comprehensive energy efficiency. The objective function is mostly the combination of economic and environmental benefits, but also ignoring the energy efficiency; (3) when dealing with the ES model, it usually considers its operating constraints, but it cannot guarantee the number and depth of its discharge, thus affecting its life expectancy; (4) due to the complexity and multiple objectives of the model, the conventional optimization algorithm is not ideal in convergence, calculation speed and initial sensitivity.

Based on the characteristics of the EI, this paper studies the system architecture, energy flow characteristics and coordinated optimization method of the regional EI. Compared with previous studies, the main contribution of this paper is as follows: Considering a CCHP-adjustable HTER, the ES life equivalent model and real-time electricity prices, a double-layer optimal scheduling model taking into account the economic benefits, environmental benefits and energy efficiency is proposed, and a particle swarm optimizer–individual variation ant colony optimization (PSO–IVACO) algorithm is used to solve the computational efficiency and accuracy. Through the calculation and simulation of the actual system, the energy savings, level of environmental protection and economic optimal dispatching schemes are realized.

2. Structure and Energy Flow Characteristics of Regional Energy Internet

Structure

According to the scale of construction, EI can be divided into region-level, city-level, national-level and global EI. Different types of EI have similarities and differences, of which the regional EI has the most basic system architecture, with the following characteristics [18,21]:

(1) The regional EI is an organic whole combined by a power grid, a thermal network, a gas network, a regional distributed energy station and an operation center;
(2) There is a variety of energy devices in the region, such as WT, PV, CCHP units, and ES equipment (including electric storage, heat storage and cold storage), to achieve a variety of energy complements;
(3) There is a wide variety of loads in addition to electric load, including heat and cold load;
(4) Information flow and energy flow are more closely linked and complex.

A regional EI system structure is shown in Figure 1.

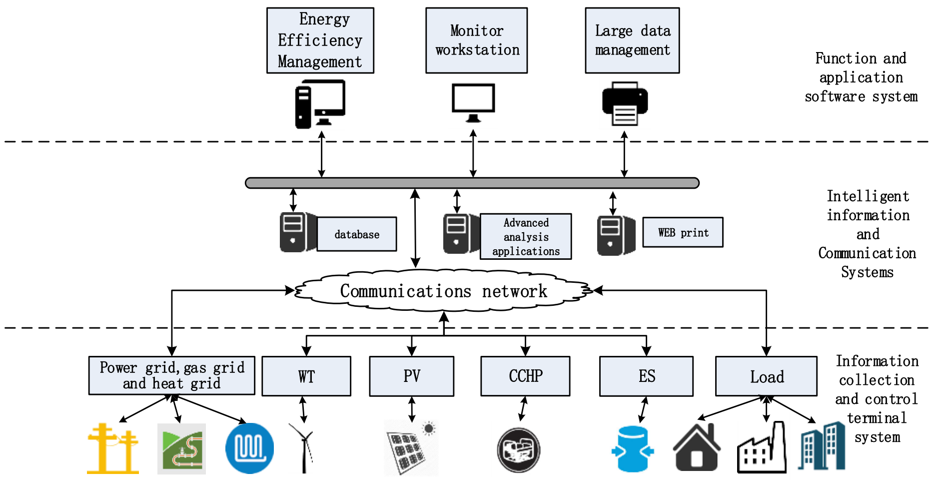

Figure 1. The structure of regional energy internet.

The energy input and output of the EI are shown in Figure 2.

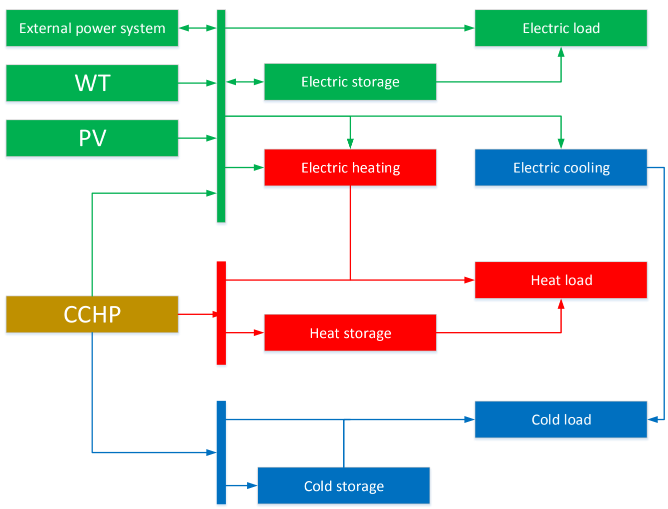

Figure 2. The flow-chart of energy flow.

In the regional EI, the electricity supply is realized by various types of distributed power supplies, storage equipment, CCHPs and electricity purchases from the outside system. The heat and cold supply is mainly supported by the CCHP, cold/heat storage equipment, or electric heating/cooling equipment. It can be seen that the ES and the CCHP are very important, as they are the key equipment to realize the mutual conversion and storage between different energy sources. Therefore, the key to realizing the optimal operation of EI lies in the development of strategies involving these two devices.

3. Coordinated Optimal Operation Model

The heat/cold equipment in the EI includes a gas boiler, the CCHP unit, absorption chillers, an electric heating/cooling device, and cold/heat storage. The electric power supply equipment includes WT, PV, the CCHP unit, ES, and purchasing extranet. Firstly, the output model and cost model of different power supply devices should be constructed. Then, the coordinated and optimized operation model is constructed.

3.1. Power Output Model and Cost Model

(1) Gas boiler model:

The amount of fuel consumed by the gas boiler is related to its thermal power:

$$Q_{boi}(t) = H_{boi}(t)\Delta t/\eta_{boi}(t) \tag{1}$$

where $Q_{boi}(t)$ is the fuel consumed in Δt period, $H_{boi}(t)$ is the thermal power, $\eta_{boi}(t)$ is the thermal efficiency of the boiler.

Gas cost is:

$$C_{boi}(t) = K_{fuel}Q_{boi}(t) \tag{2}$$

where $C_{fuel}(t)$ is the gas cost, K_{fuel} is the unit price of natural gas.

(2) CCHP model:

The CCHP unit consists of two parts: the gas generator and the waste heat boiler. The amount of fuel consumed by the electric power generation is:

$$Q_G(t) = P_G(t)\eta_G(t)\Delta t + P_{G0}(t)\eta_{G0}(t)\Delta t \tag{3}$$

where $Q_G(t)$ is the fuel consumed in Δt period, $P_G(t)$ and $P_{G0}(t)$ are the inputted natural gas power of the generator and the waste heat boiler, respectively. $\eta_G(t)$ and $\eta_{G0}(t)$ are the power conversion efficiency of the generator and the waste heat boiler, respectively.

Gas cost is:

$$C_{rs}(t) = K_{fuel}Q_G(t) \tag{4}$$

At the same time, the heat recovery system in the waste heat boiler concentrates the heat energy generated by the gas generator, and provides the thermal power as follows:

$$H_{rs}(t) = Q_G(t)(1-\eta_G(t))\eta_{rs}(t)/\Delta t \tag{5}$$

where $H_{rs}(t)$ is the thermal power and $\eta_{rs}(t)$ is the heat recovery efficiency.

Define the HTER of the CCHP unit [22]:

$$\rho(t) = \frac{H_{rs}(t)}{P_G(t)\eta_G(t) + P_{G0}(t)\eta_{G0}(t)} \tag{6}$$

As can be seen from Equation (6), under normal circumstances, when the HTER is not adjustable, the conversion efficiency cannot be changed, and $P_{G0}(t) = 0$, $\eta_{G0}(t) = 0$. The waste heat boiler can control $P_{G0}(t)$ to change the HTER. In a certain electric power output range, the CCHP's electric efficiency changes within a very small range, so the HTER will greatly affect the thermal efficiency of the system (heat-to-electric ratio adjustable principle).

However, a larger amount of fuel is not necessarily better. We need to increase the amount of fuel consumption when $P_{G0}(t)$ is increased, thus increasing the cost. When the amount of fuel increases to a certain extent, the economy will be reduced. As such, in different scheduling periods, the greatest need is to find the optimal HTER.

(3) The absorption chiller converts the heat generated by the waste heat boiler and gas boiler into cold energy:

$$H_{ac}(t) = (H^{c}_{rs}(t) + H^{c}_{boi}(t))\eta_{ac} \tag{7}$$

where $H_{ac}(t)$ is the cold power of the absorption chiller, $H^{c}_{rs}(t)$ and $H^{c}_{boi}(t)$ are the cold power provided by the waste heat boiler and gas boiler, respectively. η_{ac} is the conversion efficiency.

(4) Electric cooling/heating device model:

The cold/heat power provided by the electric cooling/heating machine is related to the power consumption and energy efficiency ratio:

$$H_{ec}(t) = P_{ec}(t)\eta_{ec} \tag{8}$$

$$H_{eh}(t) = P_{eh}(t)\eta_{eh} \tag{9}$$

where $H_{ec}(t)$ and $H_{eh}(t)$ are the cold and heat power provided by the machine, respectively. $P_{ec}(t)$ and $P_{eh}(t)$ are the corresponding power required; η_{ec} and η_{eh} are the corresponding efficiency.

(5) PV and WT model:

WT and PV are a nonlinear DC source, and the output power changes with natural conditions, which shows strong nonlinearity. In order to reach the maximum power point, the maximum power point tracking (MPPT) is required for a WT/PV generation system. The operation cost of a WT/PV can be described as follows:

$$C_{WT}(t) = K_{WT} \times P_{WT}(t) \tag{10}$$

$$C_{PV}(t) = K_{PV} \times P_{PV}(t) \tag{11}$$

where $C_{WT}(t)$ and $C_{PV}(t)$ are the operation cost of WT and PV, respectively. K_{WT} and K_{PV} are the operation management coefficient, $P_{WT}(t)$ and $P_{PV}(t)$ are the corresponding power at time t.

(6) ES model:

The remaining capacity of the ES at time t is related to the remaining capacity at time t-1 and charge/discharge capacity from t-1 to t:

$$SOC(t) = SOC(t-1) - P_{ES}(t)/\eta_{es} \tag{12}$$

where *SOC(t)* is the remaining capacity at time t; $P_{es}(t)$ is the charge/discharge power in the time period t-1, when the ES is discharging, $P_{es}(t) > 0$; when the ES is charging, $P_{es}(t) < 0$, η_{es} is the efficiency.

For the ES, its life depends on many factors, such as operating temperature, maximum charging current, and depth of discharge. The operating temperature and the charging current of the ES are usually related to their heat dispersion and control system. This paper focuses on the relationship between charging times and the charge/discharge depth. When the charge/discharge depth is R, the maximum cycle times of charging–discharging N_{ES} can be expressed as [23]:

$$N_{ES} = \alpha_1 + \alpha_2 e^{\alpha_3 R} + \alpha_4 e^{\alpha_5 R} \tag{13}$$

Where α_1~α_5 the characteristic parameters of the ES, which can be obtained from the service life test data provided by the manufacturer. When finishing a charge/discharge cycle, the ES life-loss accounts for $1/N_{ES}$ percentage of the total loss of the lifespan of the ES, and the equivalent economic loss cost C_0 is:

$$C_0 = \frac{C_{cost}}{N_{ES}} \tag{14}$$

where $C_{\cos t}$ is the initial investment cost.

Therefore, the equivalent total economic loss for the ES C_{ES} is:

$$C_{ES} = \sum_{i=1}^{N_{ES}} C_0(t) \tag{15}$$

(7) Power exchange model:

Under an electricity market environment, the EI will exchange power with an external grid; the model is as follows:

$$C_{buy} = \begin{cases} \sum_{t=1}^{T} e_1(t) \times P_{grid}(t) & , \quad P_{grid}(t) > 0 \\ 0 & , \quad P_{grid}(t) \leq 0 \end{cases} \tag{16}$$

$$C_{sold} = \begin{cases} \sum_{t=1}^{T} e_2(t) \times P_{grid}(t) & , \quad P_{grid}(t) < 0 \\ 0 & , \quad P_{grid}(t) \geq 0 \end{cases} \tag{17}$$

where C_{buy} is the purchase cost, C_{sold} is the selling income, and $P_{grid}(t)$ is the exchange power. When purchased, it is positive, and vice versa. $e_1(t)$ and $e_2(t)$ are the real-time electricity price of purchasing and selling.

3.2. Two-Layer Optimization Objective Function

The two-layer optimization model is a system optimization model with double hierarchical structure. The lower layer optimization problem is based on the scheme given by the upper decision. The optimal value of the lower decision is fed back to the upper layer and the upper layer makes a matched global optimal benefit decision according to the optimal value of the lower layer. In this paper, the upper model describes the EI energy allocation strategy, with the best economic and environmental benefits as the goal; the lower model describes the HTER strategy, with the best energy efficiency as the goal. The objective function is shown in the following Figure 3:

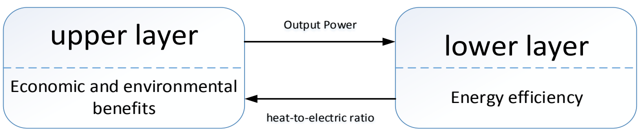

Figure 3. Two-layer optimization objective function.

The upper objective function is a combination of economic and environmental benefits:

$$f_3 = \min \sum_{t \in T} \begin{matrix} C_{boi}(t) + C_{rs}(t) + C_{WT}(t) + C_{PV}(t) \\ +C_{ES}(t) + C_{buy}(t) + C_{sold}(t) + C_{env}(t) \end{matrix} \tag{18}$$

$$C_{env}(t) = K_{gass}(Q_G(t) + Q_{G0}(t) + Q_{boi}(t)) \tag{19}$$

where K_{gass} is the cost conversion coefficient of polluted gas, $C_{env}(t)$ is the pollution discharge costs, and f_3 is a combination of economic and environmental benefits.

The optimal energy efficiency described in this paper refers to the ratio of the output energy to the input energy, indicating the utilization of the energy. The lower objective function is:

$$\max \xi = \frac{\sum P_{out}}{\sum P_{in}} = \frac{\sum (L_e(t) + L_h(t) + L_c(t))}{\sum (P_e(t) + P_h(t) + P_c(t))} \tag{20}$$

where ξ is the energy efficiency, $L_e(t)$, $L_h(t)$, $L_c(t)$ are the total output electric, heat and cold power, respectively. $P_e(t)$, $P_h(t)$, $P_c(t)$ are the total input of electric, heat and cold power, respectively.

Constraints include:

(1) As one of the key concerns regarding the implementation of the proposed method is the grid's capability to handle the operation, the condition of the power system is very important. The operation needs to satisfy the power flow constraints and static stability constraints:

(a) Power flow constraints. That is, the power output of the heat/cold/electric power and load demand should match: $L_e(t) \geq E_{load}$, $L_h(t) \geq H_{load}$, $L_c(t) \geq C_{load}$.

(b) In addition to the power flow constraints, we should also consider the grid to be in a stable operating range, which is mainly reflected in the bus voltage:

$$-0.1\text{p.u.} \leq \Delta u_i(t) \leq 0.07\text{p.u.} \tag{21}$$

where $\Delta u_i(t)$ is the voltage deviation of ith bus at time t (per unit value).

(2) Gas generator operating constraints. The power generation efficiency of the gas generator decreases with the decrease of the power, and the power consumption is reduced below the cutoff power. As such, it is necessary to limit the power generation power:

$$\varphi_{cut} P_G^{\max} \leq P_G(t) \leq P_G^{\max} \tag{22}$$

where φ_{cut} is the resection factor, $P_G^{\max}$ is the maximum power of the gas generator.

(3) Gas boiler output constraints:

$$0 \leq H_{boi}(t) \leq H_{boi}^{\max} \tag{23}$$

$$H_{boi}(t) = H_{boi}^h(t) + H_{boi}^c(t) \tag{24}$$

where $H_{boi}^{\max}$ is the maximum power of the gas boiler, $H_{boi}^h(t)$ is the thermal power output by the gas boiler.

(4) Heat recovery system constraints:

$$0 \leq H_{rs}(t) \leq H_{rs}^{\max} \tag{25}$$

$$H_{rs}(t) = H_{rs}^h(t) + H_{rs}^c(t) \tag{26}$$

where $H_{rs}^{\max}$ is the maximum power of the recovery system, $H_{rs}^h(t)$ is the thermal power output by the recovery system.

(5) Absorption chillers constraints:

$$0 \leq H_{ac}(t) \leq H_{ac}^{\max} \tag{27}$$

where $H_{ac}^{\max}$ is the maximum power of the absorption chillers.

(6) Electric cooling/heating constraints:

$$0 \leq H_{ec}(t) \leq H_{ec}^{\max} \tag{28}$$

$$0 \leq H_{eh}(t) \leq H_{eh}^{\max} \tag{29}$$

where $H_{ec}^{\max}$ and $H_{eh}^{\max}$ are the maximum power of the electric cooling/heating devices, respectively.

(7) ES constraints:

The ES working cycle is one day in duration; the energy stored on that day will be released on the same day. This is because the loss of heat and cold would be huge if long-term storage is used. Notwithstanding, the main goal of the ES is to achieve peak load in one day. So there are:

$$A(t_1) = A(t_1 + 24) \tag{30}$$

where t_1 is the starting scheduled time, A is the current capacity.

At the same time, as with all types of ES equipment, the charge and discharge power should meet the maximum constraints. Take heat storage as an example, when discharge,

$$0 \leq H_{esh}(t) \leq S_{\max}\mu \tag{31}$$

When charge,

$$0 \geq H_{esh}(t) \geq -S_{\max}\mu \tag{32}$$

where $S_{\max}$ is the maximum power of discharge/charge, μ is the maximum charge/discharge efficiency. Cold storage and electric storage are similar.

At the same time, $SOC(t)$ should meet the constraints:

$$SOC_{\min} < SOC(t) < SOC_{\max} \tag{33}$$

where $SOC_{\min}$ and $SOC_{\max}$ are the minimum constraint and maximum constraint of SOC, respectively.

(8) Tie line power constraint:

$$P_{grid}(t) \leq P_{grid,\max} \tag{34}$$

where $P_{grid,\max}$ is the transmission power limit.

3.3. Solving Algorithm

The current optimization algorithms include particle swarm optimization (PSO), ant colony optimization (ACO), artificial neural network (ANN) and genetic algorithm (GA). However, these algorithms have some flaws. For example, the ANN algorithm's generalization ability is not strong, sometimes creating overlearning; the GA is easily premature, or it is over calculated. Referring to the method in [24], we used the PSO–IVACO method to solve computational efficiency and accuracy.

Ant colony optimization (ACO) has the characteristics of self-organization and versatility, but it has the disadvantages of poor global search ability and slow searching speed. The IVACO algorithm introduces the individual population difference based on the ACO algorithm, which enhances the global search ability of the ACO algorithm. As a result of the multi-selection strategy, the individual ant mixes the cooperative path selection to avoid the premature convergence of the solution.

Due to the lack of pheromone in the initial search, the accumulation of pheromone is larger, and the search speed is slower in the IVACO algorithm. The PSO algorithm is a kind of stochastic global optimization technique; the required parameters are few, but there are early and local convergence problems. In this paper, the optimal solution of the PSO algorithm is taken as the initial solution of the IVACO algorithm and searches further for the optimal solution. The PSO–IVACO algorithm flow-chart is shown in Figure 4.

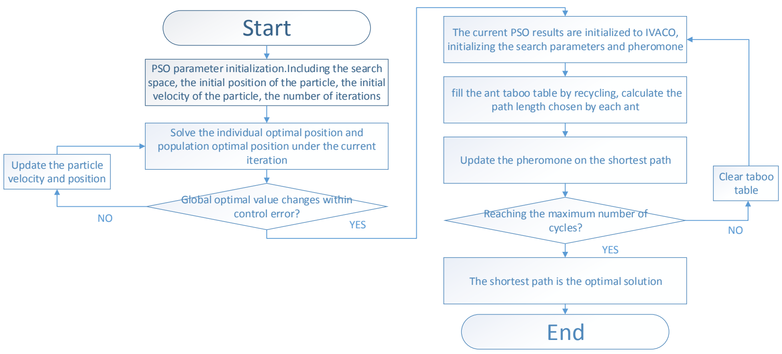

Figure 4. Particle swarm optimizer–individual variation ant colony optimization (PSO–IVACO) flow-chart.

The solution of the model is as follows:

(1) Input power matrix of load, PV, WT, and other constants. The results of the optimal scheduling at t-1 are taken as the initial value variables at t (if t = 0, then the initial value takes the last time in the previous day);
(2) PSO is used to solve iteratively. Calculate the lower target first, obtain the position and velocity of the particles, and feed back to the upper layer. Then, calculate the upper target, update the velocity and position, and feed back to the lower layer. After each iteration, perform a power flow calculation to check whether the stability constraint is met. If it is not satisfied, return to the first step, adjust the initial value. If satisfied, carry on to the next step;
(3) Repeat iterations until the objective function value changes within the control range;
(4) The optimized variable results from (2) are taken as the initial value of the IVACO iteration. Calculate by following the steps above; then, output the final result.

4. Case Study

4.1. Basic Data

The example system in this paper is based on the regional EI shown in Figure 1. We assume that the similar type of devices contained in the EI are same model. The simulation parameters used in this paper are shown in Table 1 [21–24], and the real-time electricity prices are shown in Appendix A.

Table 1. Simulation parameters.

Device	Parameters	Value
Gas generator	$P_G^{\max}$/MW	0.3
	φ_{cut}	0.25
	$\eta_G(t)$	0.85
	K_{fuel}/yuan·m^{-3}	2.28
Gas boiler	$H_{boi}^{\max}$/MW	0.5
	$\eta_{boi}(t)$	0.85
Waste heat boiler	$H_{rs}^{\max}$/MW	0.5
	$\eta_{rs}(t)$	0.60
Absorption chiller	$H_{ac}^{\max}$/MW	0.2
	$\eta_{ac}(t)$	0.80
Electric heating system	$H_{eh}^{\max}$/MW	0.3
	$\eta_{eh}(t)$	3.00
Electric cooling system	$H_{ec}^{\max}$/MW	0.3
	$\eta_{ec}(t)$	3.00
Electric energy storage	$C_{\cos t}$/yuan	200,000
	$S_{\max}$/MWh	0.4
	μ	0.2
	$A(t_1)$/MWh	0.08
	α_1	5112
	α_2	14,122
	α_3	−12,823
	α_4	5
	α_5	−3278
Heat/cold storage	$S_{\max}$/MWh	0.2
	μ	0.2
	$A(t_1)$/MWh	0
Tie line power	$P_{gird,\max}$/MW	0.1
PV	K_{PV}/yuan·MWh^{-1}	0.0096
WT	K_{WT}/yuan·MWh^{-1}	0.0108
Cost factor	K_{gass}/yuan·m^{-3}	0.95

Typical load scenarios can be divided into the heating, cooling or transition period, in which the cooling period is the most typical. At this time, the electric (E) heating (H)/cooling (C) loads both exist, and the load level is higher than the other period of this year. We selected typical days in the cooling period as an example to optimize the calculation. WT, PV and load are shown in Figure 5.

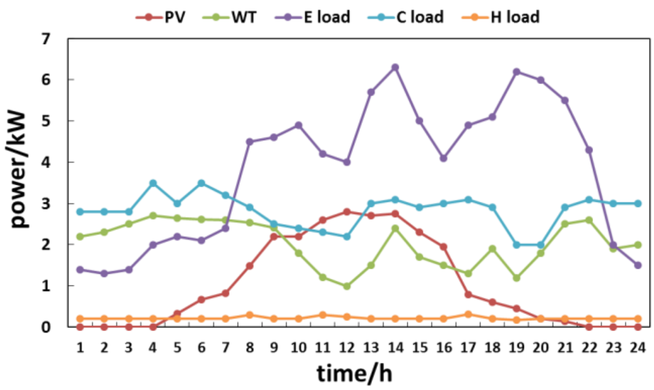

Figure 5. Power inputs of WT, PV and load.

As can be seen from Figure 5, the load of the EI exhibits obvious peak-valley characteristics (E load and C load). The peak appears at 14:00 and 19:00, which corresponds to real-time electricity prices. This feature will also profoundly affect the ES strategy.

Set the following three simulation modes:

1. Mode 1 (M1): In this situation, the CCHP unit adopts a constant HTER to supply the electric energy and heat/cold energy;
2. Mode 2 (M2): The model proposed in this paper. The CCHP unit adopts an adjustable HTER.
3. Mode 3 (M3): On the basis of M2, the ES operating cost is not included in the objective function, only taking into account its operational constraints.

4.2. Simulation Results

After calculating using the PSO–IVACO method, the optimal HTER is shown in Figure 6; the cost calculation results are shown in Figure 7; the results of energy efficiency are shown in Figure 8; and the results of the operation in one day are shown in Table 2.

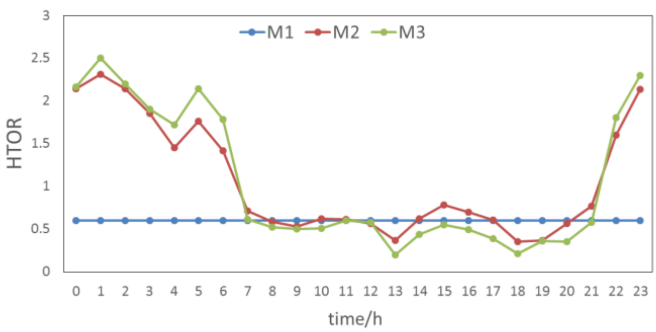

Figure 6. The optimal heat-to-electric ratio (HTER).

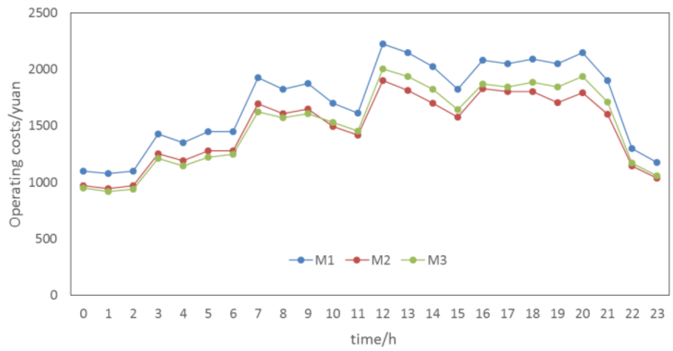

Figure 7. The operating costs.

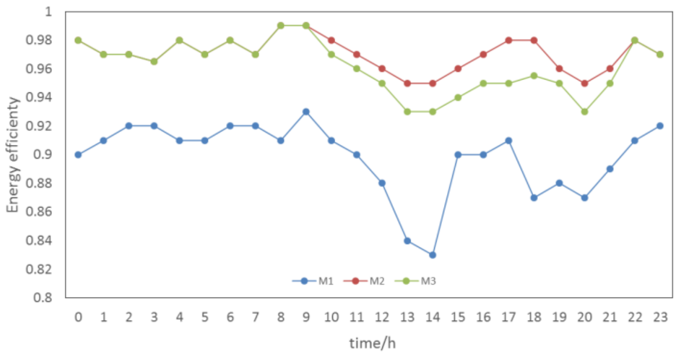

Figure 8. The energy efficiency.

Table 2. The results of the operation in one day.

Mode	Total Operating Costs/yuan	Total Energy Efficiency	ES Cost/yuan
M1	40,933.43	0.898	6218.64
M2	35,463.98	0.971	5762.14
M3	36,152.17	0.962	6125.75

Firstly, the influence of HTER on the optimal operation is analyzed:

(1) It can be seen from Figure 6 that the optimal HTER at each time is affected by the change of the heat–electric load ratio in the EI. This shows that the optimal HTER is related to the load distribution in the region.

(2) From Figures 7 and 8, and Table 2, we can determine that in the case of adjustable HTER, the CCHP unit enhances the heat power output limit, which leads to an increase in the output of the CCHP unit in the source; its operation cost and energy efficiency have improved compared with the direct use of boiler heating.

(3) From Figures 6–8, it can be found that there is a certain positive correlation between the optimal HTER and the energy efficiency, and there is a certain inverse correlation with the operation cost. When the HTER is relatively high, the energy efficiency is high and the cost is also lower. It can be concluded that by further analysis, the HTER and efficiency exist in two valley areas, namely 13:00–14:00 and 18:00–19:00. These two periods are the electric peak periods; the electric power output is high, affecting the CCHP unit thermoelectric balance ratio.

(4) The load situation has a greater impact on the operation of the EI. When the load is large, the economy and energy efficiency of the EI will be affected. Therefore, it is effective to improve the comprehensive benefit of the EI by a demand response strategy to reduce the peak and valley difference of the load.

(5) From some of the calculation results (e.g., 09:00 and 14:00), energy efficiency and economic cost are not achieving the best results simultaneously. This is due to the two-layer objective function of this paper. However, from a longer time scale, the model proposed in this paper strikes a reasonable balance between economic cost and energy efficiency, so that the calculation result of the whole day is satisfactory.

Next, we analyzed the impact of ES on scheduling. It can be seen from the curves that, due to the different ES scheduling strategies of M2 and M3, the optimal HTER, operating cost and energy efficiency are different, and the effect of energy efficiency is especially obvious. In order to better explain this problem, we took electricity storage as an example, and drew output curves within a day of M2 and M3, as shown in Figure 9.

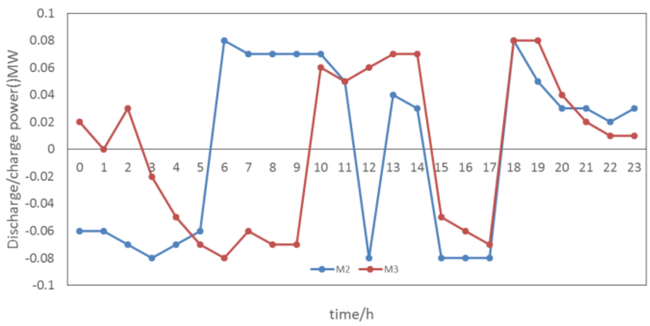

Figure 9. Charge and discharge power.

It can be seen from Figure 9, compared to M3, that the ES output in M2 is more reasonable, which is mainly reflected in:

(1) The output changes in M2 are more stable, and the charge/discharge interval is more stable and works more efficiently. This can extend its life expectancy, which also can be seen from Table 2, (the cost of ES is lower in M2);
(2) The ES strategy and real-time electricity price are more closely aligned in M2. ES discharges in the peak price and charges in the valley price. This maximization of the benefits reduces the overall operating costs;
(3) Finally, a reasonable charge/discharge of ES will ease the CCHP unit's output pressure, and optimize its operation, resulting in an improvement in energy efficiency.

In summary, the strategy proposed in this paper is more reasonable than the traditional operation method, and provides economic efficiency and high levels of environmental benefits and energy efficiency.

5. Conclusions

On the basis of the traditional distribution network optimization model, this paper studies the coordinated optimization operation strategy of the regional EI, and uses the improved PSO–IVACO algorithm to solve the issue. The research results show that compared to the traditional distribution network, the EI scheduling process is more complex, and the ES system is particularly important. At the same time, objective factors have become the key components influencing the economic operation in the system, which needs to determine the most reasonable choice that will ensure maximum benefit.

Future research directions include:

(1) Make appropriate simplifications for the optimal operation model of CCHP, and study the thermodynamic properties of the system to ensure that the optimization results will be closer to the actual project;

(2) The operational state of the regional EI is complex and changeable, and there may be some deviation in the offline scheduling strategy, and further research on the online scheduling method is needed;
(3) The proposed scheduling strategy can be used as a reference, which can be used to study the actual ES scheduling strategy.

Acknowledgments: This work was financially supported by National Natural Science Foundation (51277067) and Central University Foundation (2015XS03).

Author Contributions: Rishang Long designed the study, Rishang Long and Jian Liu performed the experiments and wrote the paper, Jianhua Zhang, Chunliang Lu and Jiaqi Shi reviewed and edited the manuscript. All authors read and approved the manuscript.

Conflicts of Interest: The authors have no conflicts of interest to declare.

Appendix A

Table A1. The spot purchase price.

Time	Price (yuan/kW·h)	Time	Price (yuan/kW·h)
1	0.240	13	0.990
2	0.177	14	1.490
3	0.130	15	0.990
4	0.096	16	0.790
5	0.030	17	0.400
6	0.170	18	0.364
7	0.271	19	0.359
8	0.386	20	0.413
9	0.516	21	0.444
10	0.526	22	0.348
11	0.810	23	0.300
12	1.000	24	0.225

Table A2. The spot sale price.

Time	Price (yuan/kW·h)	Time	Price (yuan/kW·h)
1	0.220	13	0.970
2	0.157	14	1.470
3	0.110	15	0.970
4	0.076	16	0.770
5	0.010	17	0.380
6	0.150	18	0.344
7	0.251	19	0.339
8	0.366	20	0.393
9	0.496	21	0.424
10	0.506	22	0.328
11	0.790	23	0.280
12	0.980	24	0.205

References

1. Tian, S.M.; Luan, W.P.; Zhang, D.X.; Liang, C.H.; Sun, Y.J. Technical Forms and Key Technologies on Energy Internet. *Proc. CSEE* **2015**, *35*, 3482–3495.
2. Lasseter, R.H. Micrgrids and distributed generation. *Intell. Autom. Soft Comput.* **2010**, *16*, 225–234. [CrossRef]
3. Chen, Q.X.; Liu, D.N.; Lin, J.; He, J.H.; Wang, Y. Business Models and Market Mechanisms of Energy Internet (1). *Power Syst. Technol.* **2015**, *35*, 3050–3056.

4. Tseng, Y.C.; Lee, D.; Lin, C.F.; Chang, C.Y. The Energy Savings and Environmental Benefits for Small and Medium Enterprises by Cloud Energy Management System. *Sustainability* **2016**, *8*, 531. [CrossRef]
5. Rifkin, J. The third industrial revolution. *Eng. Technol.* **2008**, *3*, 26–27. [CrossRef]
6. Siano, P. Demand response and smart grids—A survey. *Renew. Sustain. Energy Rev.* **2014**, *30*, 461–478. [CrossRef]
7. Pazouki, S.; Haghifam, M.; Moser, A. Uncertainty modeling in optimal operation of energy hub in presence of wind, storage and demand response. *Int. J. Electr. Power Energy Syst.* **2014**, *61*, 335–345. [CrossRef]
8. Yang, F.; Bai, C.F.; Zhang, Y.B. Research on the value and implementation framework of energy internet. *Proc. CSEE* **2015**, *35*, 3495–3502.
9. Zeng, M.; Yang, Y.Q.; Liu, D.N.; Zeng, B.; Ouyang, S.J.; Lin, H.Y.; Han, X. "Gen-eration-Grid-Load-Storage" Coordinative Optimal Opera-tion Mode of Energy Internet and Key Technologies. *Power Syst. Technol.* **2016**, *40*, 114–125.
10. Lee, E.K.; Shi, W.; Gadh, R.; Kim, W. Design and Implementation of a Microgrid Energy Management System. *Sustainability* **2016**, *8*, 1143. [CrossRef]
11. Song, N.O.; Lee, J.H.; Kim, H.M. Optimal Electric and Heat Energy Management of Multi-Microgrids with Sequentially-Coordinated Operations. *Energies* **2016**, *9*, 473. [CrossRef]
12. Yan, B.; Wang, B.; Zhu, L.; Liu, H.; Liu, Y.L.; Ji, X.P.; Liu, D.C. A Novel, Stable, and Economic Power Sharing Scheme for an Autonomous Microgrid in the Energy Internet. *Energies* **2015**, *8*, 12741–12764. [CrossRef]
13. Li, Y.S. Scheduling Optimization and Real-time Control Method for Micro-Grids Interconnection. Master's Thesis, North China Electric Power University, Beijing, China, 2016.
14. Saponara, S.; Araneo, R. Distributed Measuring System for Predictive Diagnosis of Uninterruptible Power Supplies in Safety-Critical Applications. *Energies* **2016**, *9*, 327. [CrossRef]
15. Sergio, S.; Luca, F.; Fabio, B. Predictive Diagnosis of High-Power Transformer Faults by Networking Vibration Measuring Nodes with Integrated Signal Processing. *IEEE Trans. Instrum. Meas.* **2016**, *8*, 1749–1760.
16. Sergio, S.; Tony, B. Network Architecture, Security Issues, and Hardware Implementation of a Home Area Network for Smart Grid. *J. Comput. Netw. Commun.* **2012**, *2012*, 534512.
17. Alex, Q.H.; Mariesa, L.C.; Gerald, T.H.; Jim, P.Z.; Steiner, J.D. The Future Renewable Electric Energy Delivery and Management (FREEDM) System: The Energy Internet. *Proc. IEEE* **2011**, *99*, 133–148.
18. Evins, R.; Orehounig, K.; Dorer, V.; Carmeliet, J. New formulations of the 'energy hub' model to address operational constraints. *Energy* **2014**, *73*, 387–398. [CrossRef]
19. Hadis, M.; Amir, A.; Mahdi, E. Optimal operation of a multi-source microgrid to achieve cost and emission targets. In Proceedings of the 2016 IEEE Power and Energy Conference at Illinois (PECI), Urbana, IL, USA, 19–20 February 2016; pp. 1–6.
20. Moradi, H.; Moghaddam, I.; Gerami, M.M. Opportunities to Improve Energy Efficiency and Reduce Greenhouse Gas Emissions for a Cogeneration Plant. In Proceedings of the IEEE International Energy Conference and Exhibition, Manama, Bahrain, 18–22 December 2010; pp. 785–790.
21. Sheikhi, A.; Ranjbar, A.M.; Oraee, H.; et al. Optimal operation and size for an energy hub with CCHP. *Energy Power Eng.* **2011**, *3*, 641–649.
22. Shi, J.Y.; Xu, J.; Zeng, B.; Zhang, J.H. A Bi-Level Optimal Operation for Energy Hub Based on Regulating Heat-to-Electric Ratio Mode. *Power Syst. Technol.* **2016**, *40*, 2960–2968.
23. Shen, Y.M.; Hu, B.; Xie, K.G. The optimal eco-nomic operation of the isolated microgrid with the loss of energy storage life. *Power Grid Technol.* **2014**, *38*, 2372–2378.
24. Zeng, M.; Han, X.; Li, R.; Li, Y.F.; Peng, L.L.; Li, N. Multi-Energy Synergistic Optimization Strategy of Micro Energy Internet with Supply and Demand Sides Considered and Its Algorithm Utilized. *Power Grid Technol.* **2017**, *41*, 409–418.